SUPPLEMENT TO THE *WELDING JOURNAL,* NOVEMBER 2007
Sponsored by the American Welding Society and the Welding Research Council

Fusion-Boundary Macrosegregation in Dissimilar-Filler Metal Al-Cu Welds

Two recently proposed macrosegregation mechanisms have been verified by microstructure examination and composition measurements of Al-Cu welds

BY Y. K. YANG AND S. KOU

ABSTRACT. Dissimilar filler metals, that is, filler metals different from the base metal in composition, are routinely used in arc welding but macrosegregation can form and degrade the weld quality. Based on the liquidus temperatures of the weld metal (T_{LW}) and the base metal (T_{LB}) as well as the stagnant or laminar-flow layer of liquid base metal along the weld pool boundary suggested by Savage, two new mechanisms have been proposed recently for macrosegregation near the fusion boundary in arc welds made with dissimilar filler metals, one for $T_{LW} < T_{LB}$ and the other $T_{LW} > T_{LB}$. To verify the mechanisms, the binary Al-Cu system was selected, and gas metal arc welding was used. In the case of $T_{LW} < T_{LB}$, 1100 Al (commercially pure Al) was selected as the base metal because pure Al has the highest liquidus temperature and thus $T_{LW} < T_{LB}$ is met automatically. It was welded with filler metal 2319 Al (Al-6.3Cu) and Al/Cu composite filler metals of higher Cu contents. Features including beaches, peninsulas, and islands were found along the fusion boundary. The beaches were thin and discontinuous, and the peninsulas and islands roughly parallel to the fusion boundary. These features were pure Al, that is, they originated from the liquid base metal that solidified without mixing with the bulk weld pool. In the case of $T_{LW} > T_{LB}$, on the other hand, the Al-33Cu eutectic was selected as the base metal because the eutectic has the lowest liquidus temperature and thus $T_{LW} > T_{LB}$ is met automatically. It was welded with filler metal 1100 Al. The beach along the fusion boundary was significantly thicker and more continuous than those with $T_{LW} < T_{LB}$. It was intruded by the weld metal, with peninsulas, and islands randomly oriented in the space between the weld-metal intrusions. These beach, peninsulas and islands were eutectic, that is, they originated from the liquid base metal that solidified without mixing with the bulk weld pool. In either case, the filler-deficient zone was thicker in welds made with a larger difference between T_{LW} and T_{LB}. All these observations were consistent with and thus verified the proposed mechanisms.

Y. K. YANG, Graduate Student, and S. KOU, Professor, are with the Department of Materials Science and Engineering, University of Wisconsin, Madison, Wis.

Introduction

In arc welding the filler metal is often dissimilar, that is, different from the workpiece in composition, in order to prevent cracking or to develop desired physical or chemical properties. Macrosegregation can exist near the fusion boundary of welds made with dissimilar filler metals and degrade the weld quality (Refs. 1–17).

In addition to the stagnant or laminar-flow layer of liquid base metal along the weld pool boundary suggested by Savage (Ref. 3), Kou and Yang (Ref. 18) have recently considered the liquidus temperatures of the weld metal T_{LW} and the base metal T_{LB} and proposed two new mechanisms for fusion-boundary macrosegregation in arc welds made with dissimilar filler metals, one for $T_{LW} < T_{LB}$ and the other $T_{LW} > T_{LB}$. They described how filler-deficient peninsulas and islands as well as beaches can form along the resultant fusion boundary. The characteristics of the beaches, peninsulas, and islands formed by these two mechanisms can be distinctly different, as is described subsequently.

KEYWORDS

Al-Cu Welds
Dissimilar Filler Metal
Filler Metal
Liquidus Temperature
Macrosegregation

Experimental Procedure

The Al-Cu system was selected for the present study for the following reasons. First, it is a simple binary alloy system with a well-documented phase diagram for determining the liquidus temperature from the alloy composition. Second, Al-Cu alloys are useful light structural materials, such as 2219 Al (Al-6.3Cu) and 2214 Al (essentially Al-4.4Cu). Third, casting Al-Cu alloys is straightforward, requiring no special protection against oxidation or fire (as in casting Mg alloys). Fourth, pure Al and Cu wires are readily available and deformable.

Plates of both 1100 Al (commercially pure aluminum) and Al-33Cu eutectic were welded (all Cu contents in the present study in wt-%). They were both 9.5 mm (⅜ in.) thick, 102 mm (4 in.) wide, and 102 mm (4 in.) long. The eutectic alloy was prepared by casting. Predetermined quantities of 99.99% Al and a master alloy of Al-50.86Cu were induction melted in a graphite crucible and cast at 700° to 750°C into a graphite mold.

Filler metals of various Cu contents were used, including 1100 Al, 2319 Al (Al-6.3Cu), Al-30.5Cu, and Al-52.5Cu. The last two materials are not commercially available. The Al-30.5Cu welding wire was fabricated from a four-strand composite of three commercially pure Al (1100 Al) wires of 0.81 mm diameter and one 99.99% purity Cu wire of 0.51 mm diameter, twisted together and then pulled to straighten. The density of pure Al is 2.70

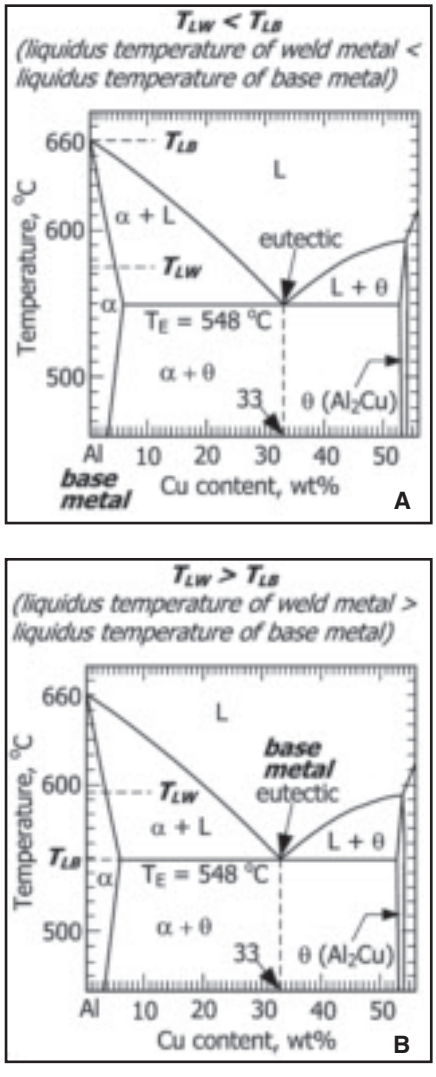

Fig. 1 — Aluminum-rich side of binary Al-Cu phase diagram (Ref. 20) and selection of base metal for welding. A — Pure Al as base metal and thus $T_{LW} < T_{LB}$; B — Al-33Cu eutectic as base metal and thus $T_{LW} > T_{LB}$.

g/cm³ and that of pure Cu 8.96 g/cm³. Thus, the Cu content of the composite welding wire $(\text{wt-\% Cu})_{\text{filler}} = 100 \times 8.96\, A_{Cu} / (8.96\, A_{Cu} + 3 \times 2.70\, A_{Al})$, where A_{Cu} is the cross-sectional area of the pure Cu wire and A_{Al} that of the pure Al wire. Since $A_{Al} = \pi(0.81\text{ mm})^2/4 = 0.515\text{ mm}^2$ and $A_{Cu} = \pi(0.51\text{ mm})^2/4 = 0.204\text{ mm}^2$, $(\text{wt-\% Cu})_{\text{filler}} = 30.5$.

The Al-52.5Cu welding wire was also fabricated from a four-strand composite made by twisting together three pure Al wires and one pure Cu wire, but all wires were 0.81 mm in diameter. Since $A_{Al} = A_{Cu} = 0.515\text{ mm}^2$, $(\text{wt-\% Cu})_{\text{filler}} = 52.5$. The overall diameter was about 1.9 mm for both composite wires.

The advantage of composite wires is that filler metals of high Cu contents can be prepared easily. The disadvantage of this approach, however, is that gas porosity is higher in the resultant weld metal

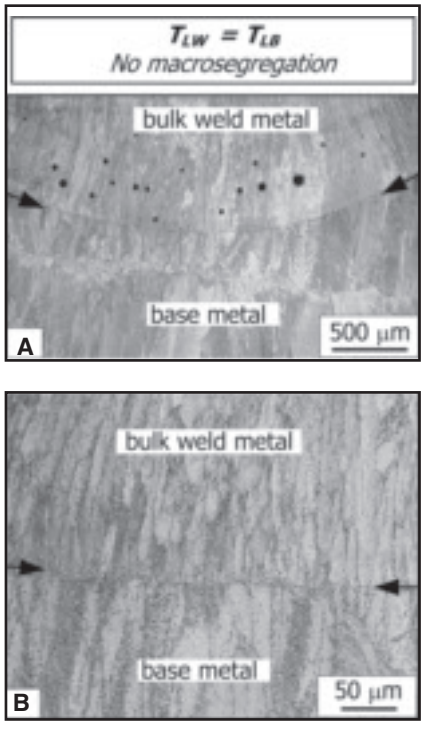

Fig. 2 — Transverse micrographs showing no macrosegregation when essentially $T_{LW} = T_{LB}$. A — Near weld bottom; B — enlarged. Both base metal and weld metal are essentially Al-33Cu (both eutectic when viewed at higher magnifications). Arrows indicate fusion boundary.

probably because of some air trapped in the space between individual wires.

Bead-on-plate welds with partial penetration were made by gas metal arc welding (GMAW). Commercial filler metals 1100 Al and 2319 Al were used, the former for the Al-33Cu eutectic plates and the latter for the 1100 Al plates. The wire diameter was 1.2 mm (3/64 in.). The welding conditions were as follows: 25–28 V, 169–212 mm/s (400–500 in./min) wire feeding speed, 6.4–8.5 mm/s (15–20 in./min) travel speed, and 280–285 A average current. Composite wires Al-52.5Cu and Al-30.5Cu were used for welding the 1100 Al plates. The welding conditions were as follows: 25 V, 85–106 mm/s (200–250 in./min) wire feeding speed, 4.2–8.5 mm/s (10–20 in./min) travel speed, and 260–285 A average current. As compared to the commercial wires 1100 Al and 2319 Al, the wire feeding speed was lower with the composite wires because of their larger diameter. Regardless of which wire was used, the contact tube to workpiece distance was about 19.1 mm (¾ in.), and the torch was held perpendicular to the workpiece.

The resultant welds were cut, polished and etched with a solution of 0.5 vol-% HF in water for microstructural examination by optical microscopy. Macrographs of cross sections of the welds were taken with a digital camera.

The Cu content in a homogeneous Al-Cu weld can be calculated as follows (Ref. 19):

$$(\text{wt-\% Cu})_{\text{weld}} = (\text{wt-\% Cu})_{\text{base}} \times [A_b/(A_b + A_f)] + (\text{wt-\% Cu})_{\text{filler}} \times [A_f/(A_b + A_f)] \quad (1)$$

where A_b and A_f are the areas in the weld transverse cross section that are below and above the workpiece surface, respectively. With macrosegregation limited to near the fusion boundary, such as the welds in the present study, the composition of the bulk weld metal can still be calculated using Equation 1, as an approximation. In Equation 1 areas A_b and A_f represent contributions from the base metal and filler metal, respectively. The ratio $A_b/(A_b + A_f)$ is the so-called dilution ratio. Areas A_b and A_f were determined by enlarging the transverse macrograph on a computer monitor and by using commercial computer software.

For welds with high Cu contents, the difference between the density of Cu (ρ_{Cu} = 8.96 g/cm³) and that of Al (ρ_{Al} = 2.70 g/cm³) can be significant. This density difference can be considered in the calculation of the weld-metal Cu content by using the following equation derived in Appendix A:

$$(\text{wt-\% Cu})_{\text{weld}} = 100\, R\, \rho_{Cu} / [R\, \rho_{Cu} + (1 - R)\, \rho_{Al}] \quad (2)$$

where

$$R = \{(\text{wt-\% Cu}/\rho_{Cu}) / [(\text{wt-\% Cu}/\rho_{Cu}) + (100 - \text{wt-\% Cu})/\rho_{Al}]\}_{\text{base}} \times [A_b/(A_b + A_f)] + \{(\text{wt-\% Cu}/\rho_{Cu}) / [(\text{wt-\% Cu}/\rho_{Cu}) + (100 - \text{wt-\% Cu})/\rho_{Al}]\}_{\text{filler}} \times [A_f/(A_b + A_f)] \quad (3)$$

Again, with macrosegregation limited to near the fusion boundary, the Cu content of the bulk weld metal can be calculated using Equation 2 as an approximation. With $\rho_{Al} = \rho_{Cu} = \rho$, Equation 3 reduces to

$$R = (\text{wt-\% Cu}/\rho)_{\text{base}} \times [A_b/(A_b + A_f)] + (\text{wt-\% Cu}/\rho)_{\text{filler}} \times [A_f/(A_b + A_f)] \quad (4)$$

Upon substituting Equation 4 and $\rho_{Al} = \rho_{Cu} = \rho$, Equation 2 reduces to Equation 1. Thus, Equation 1 is a special case of Equation 2 when the densities of all elements involved are identical.

As mentioned before, the Al-33Cu eutectic plates were welded with filler metal

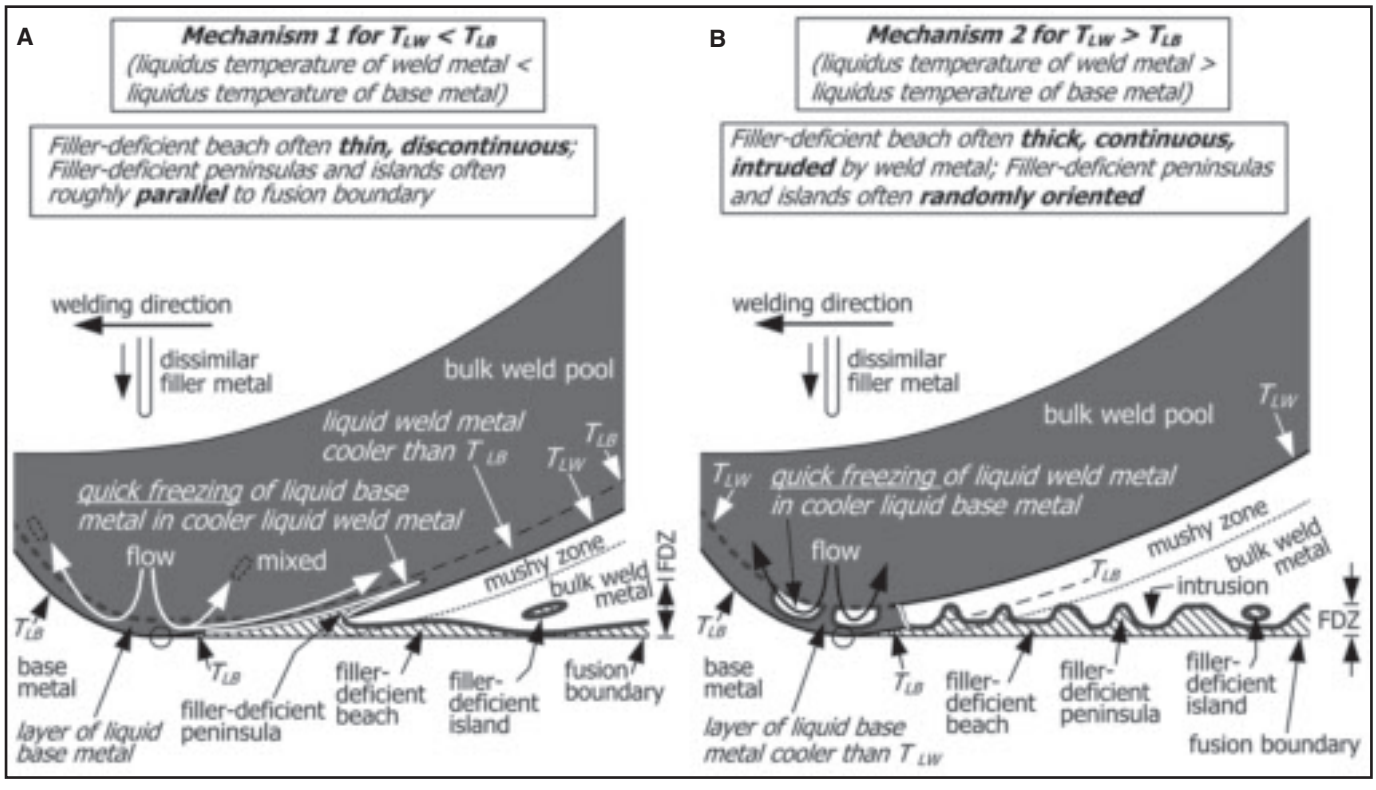

Fig. 3 — Mechanisms of fusion-boundary macrosegregation (formation of filler metal-deficient zone FDZ). A — Mechanism 1 for $T_{LW} < T_{LB}$; B — Mechanism 2 for $T_{LW} > T_{LB}$. Pool boundary is melting front before circle and solidification front after. From Kou and Yang (Ref. 18).

Equation 2 when the densities of all elements involved are identical.

As mentioned before, the Al-33Cu eutectic plates were welded with filler metal 1100 Al. In one experiment the weld-metal Cu content was further reduced by placing before welding a rectangular rod of 1100 Al in a rectangular groove at the workpiece top surface along the welding path. The rod and the groove were both 2 × 8 mm in transverse cross section. The rod was completely melted and mixed in the weld pool during welding.

The composition profiles across the fusion boundary were determined by EDS (energy-dispersive spectroscopy) during SEM (scanning electron microscopy).

Results and Discussion

For convenience of discussion, the Al-rich side of the binary Al-Cu phase diagram is shown in Fig. 1 (Ref. 20). Pure Al solidifies at the melting point 660°C and the eutectic, Al-33Cu, solidifies at the eutectic temperature 548°C, with a lamellar structure of α-Al and θ-Al_2Cu. Thus, the highest liquidus temperature is the melting point of pure Al 660°C, and the lowest one the eutectic temperature 548°C.

In order to test the proposed mechanisms, it is desirable to have a large difference between the liquidus temperature of the base metal T_{LB} and the liquidus temperature of the weld metal T_{LW} so that the effect of this temperature difference on solidification and macrosegregation can be significant enough to be examined clearly. The maximum possible difference between T_{LB} and T_{LW} for the binary Al-Cu system is 112°C (660°C – 548°C).

No Filler Metal-Deficient Zone in Welds with $T_{LW} = T_{LB}$

Figure 2 shows the transverse micrographs of a weld made on Al-33Cu eutectic with composite welding wire Al-31Cu. From Equation 2, the 60.8% dilution of the weld, and the compositions of the base metal and the filler metal, the weld metal composition was Al-32Cu. Dendrites of the Al-rich α phase were found occasionally in the bulk weld metal (but not in the area shown in Fig. 2) because Al-32Cu was just slightly lower in Cu than the eutectic composition Al-33Cu. Other than these, the weld metal was eutectic just like the base metal, and as an approximation, $T_{LW} = T_{LB}$.

Figure 2 indicates two things. First, the composite wire worked properly — no evidence of unmixed or unmelted Cu because of the much higher melting point of Cu (1085°C) than Al (660°C). Second, there was no evidence of beaches, peninsulas, or islands along the fusion boundary (indicated by two arrows) or elsewhere in the bulk weld metal. The weld metal grains appeared to grow normal to the fusion boundary.

Filler Metal-Deficient Zone in Welds with $T_{LW} < T_{LB}$

For convenience of discussion, the mechanisms proposed recently for fusion-boundary macrosegregation, that is, formation of the filler metal-deficient zone (FDZ), in dissimilar filler-metal welds are shown in Fig. 3 (Ref. 18). Here the filler metal mixes completely with the homogeneous bulk weld pool. The more complicated case where the filler metal mixes only partially with the bulk weld pool before reaching the bottom of the weld pool is considered in a follow-up paper (Ref. 21).

Mechanism 1, shown in Fig. 3A, is for filler metals that make $T_{LW} < T_{LB}$. According to fluid mechanics (Ref. 22), the velocity of a moving liquid is zero at a solid wall, that is, the so-called "no-slip" boundary condition for fluid flow. Thus, near the weld pool boundary convection is weakened, and a stagnant or laminar-flow layer of liquid base metal can exist as Savage

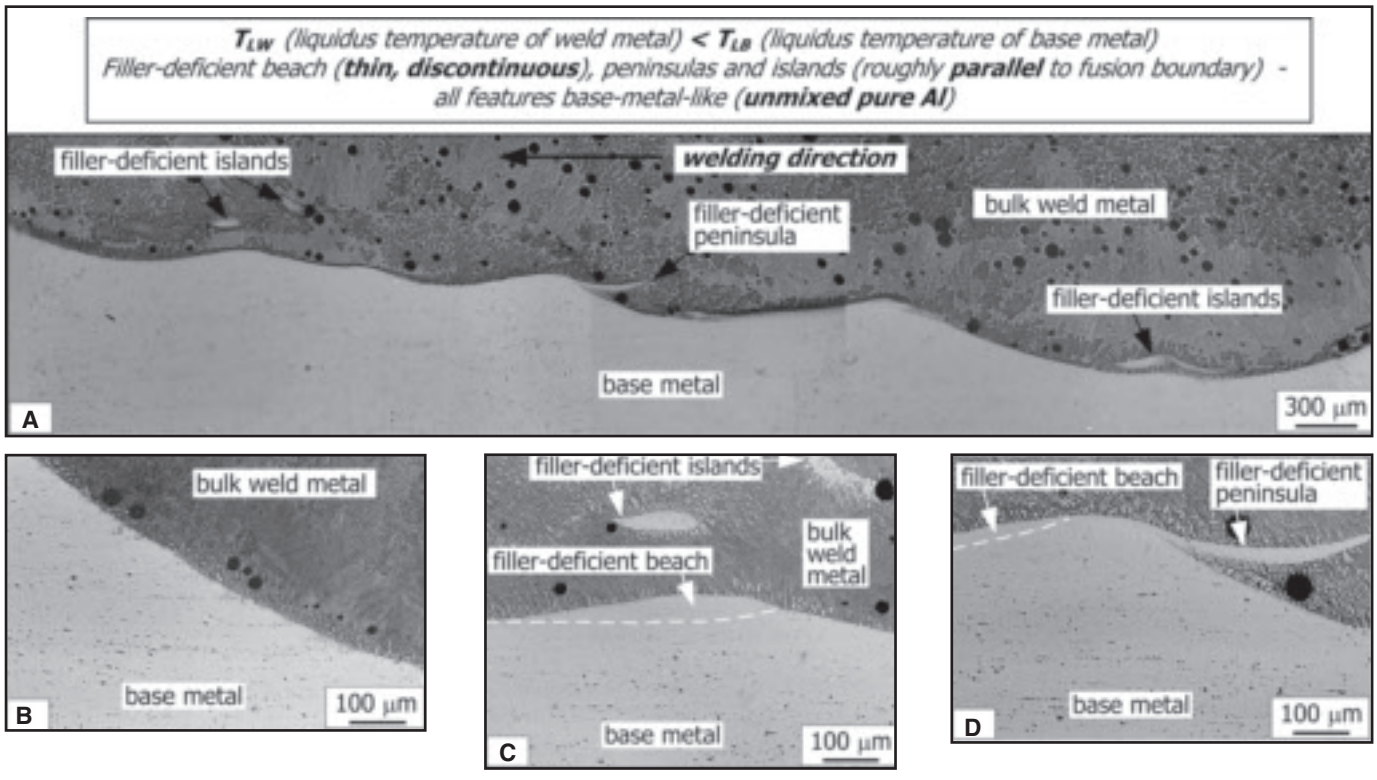

Fig. 4 — Longitudinal micrographs for $T_{LW} < T_{LB}$. A — Overview; B — melting front; C, D — weld bottom. Base metal: 1100 Al (pure Al); weld metal: Al-33Cu; T_{LW} = 548°C and T_{LB} = 660°C. Beaches, peninsulas, and islands all appeared pure Al like base metal, suggesting they originated from unmixed base metal.

suggested (Ref. 3).

The solidification front is no longer isothermal as in welding without a dissimilar filler metal. In Fig. 3 the portion of the weld pool boundary behind the circle is the solidification front and that ahead of it is the melting front. As shown, the solidification front is T_{LW} for the bulk weld pool but T_{LB} for the liquid base metal solidifying near the fusion boundary. The liquid weld metal in the region immediately ahead of the solidification front is below T_{LB}. This is only because of $T_{LW} < T_{LB}$ and not any undercooling. The liquid base metal in the stagnant or laminar-flow layer swept by convection into this cooler region can freeze quickly without much mixing with the surrounding liquid and form filler-metal-deficient peninsulas or islands. The peninsulas often tend to be roughly parallel to the fusion boundary. The islands can also be roughly parallel to the fusion boundary unless they happen to rotate before the surrounding liquid in the cooler region solidifies.

The liquid base metal remaining in the layer can solidify as a filler-deficient beach along the weld interface, often thin and discontinuous because of weld pool convection. These features of beaches, peninsulas, and islands are filler-deficient because of no or partial mixing with the bulk weld pool, in which the filler metal is uniformly distributed during welding. The larger the temperature difference ($T_{LB} - T_{LW}$) is, the thicker the resultant FDZ can be, but the actual thickness also depends much on the direction and strength of weld pool convection.

A number of factors are considered as follows. First, the liquid base metal is carried into the cooler region with sensible heat. However, the sensible heat is expected to be small because of the small amount of liquid base metal carried into the cooler region. Thus, the liquid base metal can freeze quickly before much mixing occurs. Second, the closer the solidus temperature of the liquid base metal is to its liquidus temperature, the more quickly freezing can progress appreciably. Third, a liquid base metal with a lower density than the bulk weld metal has a tendency to float upward into and mix with the bulk weld pool above it, for instance, a thin layer of liquid pure Al base metal under an Al-Cu bulk weld pool. This might contribute to the thin and discontinuous Al-rich beach in a pure Al weld made with Al-Cu filler metals. Fourth, the viscosity of the liquid base metal can differ from that of the bulk weld metal. The former can have a lower temperature and thus a higher viscosity though the composition difference between the two may also play a role. A higher viscosity may help the liquid base metal layer stick better to the unmelted solid base metal.

The condition of $T_{LW} < T_{LB}$, as shown in Fig. 1A, can be met automatically by using 1100 Al (essentially pure Al) as the base metal because the highest achievable liquidus temperature of aluminum alloys is the melting point 660°C. An advantage of using 1100 Al is that its microstructure is featureless (that is, without the cells or dendrites in Al-Cu alloys) and hence easy to recognize. To keep the temperature difference ($T_{LW} - T_{LB}$) large, T_{LW} can be kept low by using high-Cu welding wires to keep the weld-metal Cu content high.

Figure 4 shows longitudinal micrographs taken along the central plane of a weld made on 1100 Al with filler metal Al-52.5Cu. Figure 4A shows the overall microstructure along the bottom of the weld, the welding direction being from right to left. As shown, the peninsulas and islands are roughly parallel to the fusion boundary. Figure 4B shows the microstructure somewhere along the melting front. Figure 4C and D show, respectively, two islands and one peninsula in Figure 4A at a higher magnification.

The dilution of the weld was about 48%, and the weld metal composition was about Al-33Cu (from Equation 2), that is, the eutectic composition. From the Al-Cu phase diagram (Fig. 1A), the liquidus tem-

perature of the weld metal, T_{LW}, was the eutectic temperature 548°C. Taking the base metal 1100 Al as pure Al as an approximation, the liquidus temperature of the base metal, T_{LB}, was the melting point of pure Al 660°C. Thus, T_{LW} was well below T_{LB} and the temperature difference ($T_{LB} - T_{LW}$) was 112°C.

The filler-deficient beaches, peninsulas, and islands in Fig. 4C and D were similar to the base metal in microstructure except without the particles of dark-etching Al-Fe intermetallic compounds in the base metal. Further etching (for minutes) and higher magnifications confirmed that these compounds were redistributed by solidification as very fine dots or short line segments lining up along the cell boundaries of the cellular structure in the beaches, peninsulas, or islands. The broken lines in Fig. 4C and D were drawn along the boundaries of the regions in which such dots or line segments existed, that is, the beaches. Unfortunately, long etching often degraded the overall quality of the micrographs significantly as can be seen subsequently in Fig. 5A.

The peninsula (Fig. 4D) is roughly parallel to the fusion boundary, especially the part of the fusion boundary to the left of the peninsula, where it originated during welding. The islands (Fig. 4C) are also roughly parallel to the fusion boundary. These findings are consistent with the proposed mechanism. The porosity in the weld metal was probably caused by some air trapped in the space between individual wires in the composite welding wire.

Figure 5 shows the transverse micrographs of welds made on 1100 Al with filler metals of various Cu contents. The first micrograph (Fig. 5A) was taken from a weld made with welding wire 2319 Al (Al-6.3Cu). The dilution was 51%, and the weld metal composition was Al-3.0Cu. From the Al-Cu phase diagram, T_{LW} = 653°C. Since T_{LB} = 660°C, T_{LW} was below T_{LB} and ($T_{LB} - T_{LW}$) = 7°C. The second micrograph (Fig. 5B) was taken from a weld made with filler metal Al-31Cu. The dilution was 29%, and the weld-metal composition was Al-23Cu. From the Al-Cu phase diagram, T_{LW} = 589°C. Thus, T_{LW} was below T_{LB} and ($T_{LB} - T_{LW}$) = 71°C. The last two micrographs (Fig. 5C and D) were taken at two different locations along the weld shown previously in Fig. 4, that is, 1100 Al welded with filler metal Al-52.5Cu. As mentioned before, T_{LW} = 548°C and T_{LB} = 660°C. Thus, T_{LW} was below T_{LB} and ($T_{LB} - T_{LW}$) = 112°C.

Three observations can be made regarding the filler metal-deficient zone (FDZ) in the micrographs in Fig. 5. The FDZ can be defined as the region of the weld metal along the fusion boundary that contains all the filler metal-deficient features present in the weld metal (such as beaches, peninsulas, and islands), between the fusion boundary and a boundary that is parallel to and just far enough from the fusion boundary to include all the features. First, these beaches, peninsula, and islands are light-etching just like the base metal, suggesting that they had originated from the base metal that was melted but not mixed with the bulk weld pool. In Fig. 5A the very fine dark-etching lines in the beach are somewhat normal to the fusion boundary (the white broken line). Likewise, in Fig. 5B, the dark-etching grain boundary in the beach is normal to the fusion boundary (the white broken line). These both indicate that the beaches are indeed solidification structure and that the dark-etching particles of Al-Fe intermetallic compounds originally in the base metal were redistributed during solidification along the cell or grain boundaries. Second, the peninsulas and island were roughly parallel to the fusion boundary, which is consistent with the mechanism proposed for $T_{LW} < T_{LB}$ — Fig. 3A. Third, the FDZ increased in thickness with increasing temperature difference ($T_{LB} - T_{LW}$), which is also consistent with Mechanism 1. Before leaving the present paragraph, it is worth mentioning that the bulk weld metal in Fig. 5A was overetched and became blurred because of the long etching needed to bring out the cellular structure of the beach.

Figure 6 shows a composition profile taken along path AE across the fusion boundary and the island shown in Fig. 5D. The Cu content at the core of the island was essentially zero, identical to that of the base metal. This confirms that the island originated from the liquid base metal that froze quickly without mixing with the liquid weld metal. This is consistent with the proposed theory. The measured weld-metal composition was about Al-35Cu, close to that of Al-33Cu calculated based on the dilution ratio and Equation 2. Composition gradients existed between the island core and the adjacent weld metal. The gradients are likely to be associated with diffusion or partial mixing between the liquid base metal and the liquid weld metal and with solute segregation during solidification, as suggested by Mechanism 1.

This composition profile shows another advantage of selecting pure aluminum as the base metal, that is, the composition profile in pure Al (including the base metal and the island) is easy to measure by EDS because it is uniform. If any alloy workpiece, for instance, Al-6Cu, had been used, the composition would have fluctuated wildly across the island due to

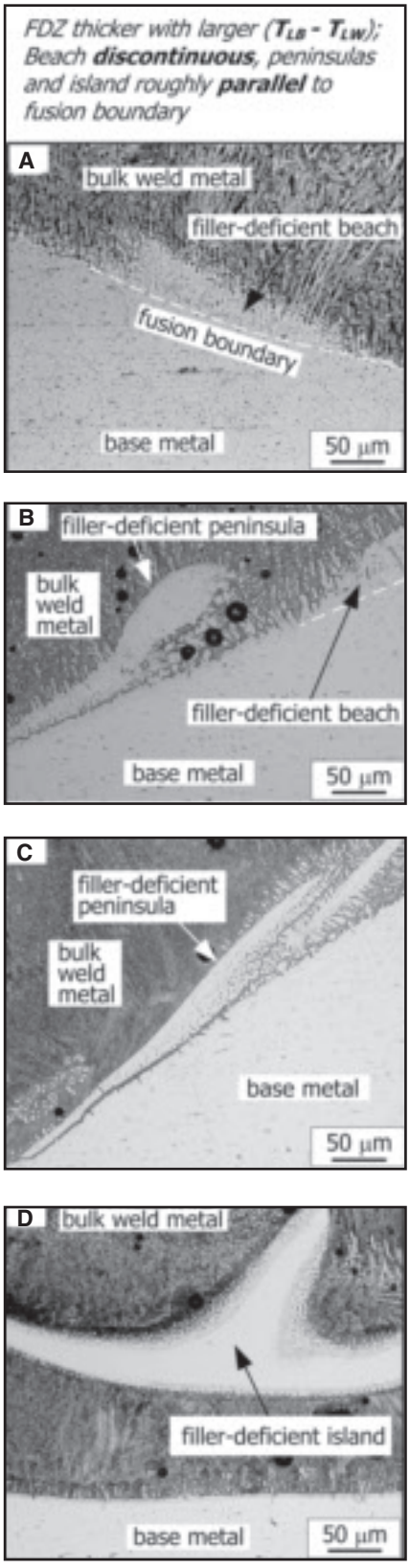

Fig. 5 — Transverse micrographs showing effect of ($T_{LB} - T_{LW}$) on thickness of filler metal-deficient zone (FDZ). A — ($T_{LB} - T_{LW}$) = 7°C; B — ($T_{LB} - T_{LW}$) = 71°C; C, D — ($T_{LB} - T_{LW}$) = 112°C. Base metal: 1100 Al (pure Al).

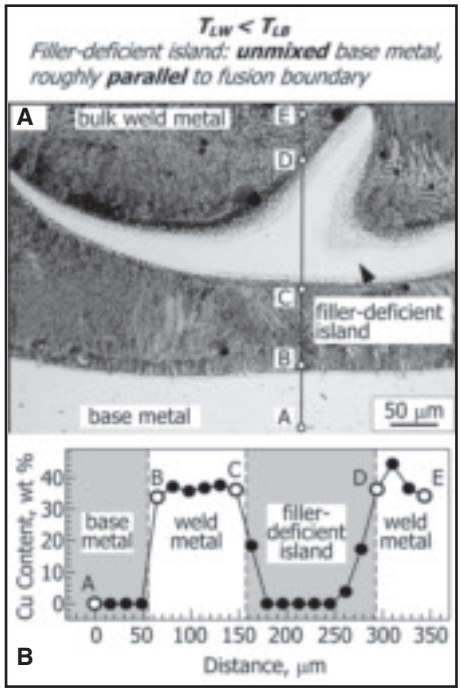

Fig. 6 — Macrosegregation across fusion boundary when $T_{LW} < T_{LB}$. A — Transverse micrograph; B — composition profile. Base metal: 1100 Al (pure Al); weld metal: Al-33Cu. Core of island identical to base metal in composition, i.e., unmixed base metal.

microsegregation across dendrite arms.

Filler-Metal-Deficient Zone in Welds with $T_{LW} > T_{LB}$

Mechanism 2, shown in Fig. 3B, is for filler metals that make $T_{LW} > T_{LB}$ (Ref. 18). The base metal next to the boundary of the homogeneous bulk weld pool (which is at T_{LW}) is above T_{LB} and thus must form a liquid layer because $T_{LW} > T_{LB}$ regardless of the extent of weld pool convection. Since the layer of liquid base metal near the fusion boundary is below T_{LW}, the liquid weld metal pushed by convection into this cooler region can freeze quickly as intrusions without much mixing with the liquid base metal. This also means that the liquid base metal in the layer solidifies without much mixing. The result is a filler-deficient beach with weld-metal intrusions. The liquid base metal that solidifies in the space between intrusions can appear as peninsulas or even islands near the fusion boundary. Since the flow of the liquid weld metal into the layer of liquid base metal during welding may be random, the peninsulas and islands can be randomly oriented instead of roughly parallel to the fusion boundary as in the case of $T_{LW} < T_{LB}$. The larger the temperature difference ($T_{LB} - T_{LW}$) is, the thicker the FDZ can be, but the actual thickness can also be affected by the direction and strength of weld pool convection.

The condition of $T_{LW} > T_{LB}$, as shown in Fig. 1B, can be met automatically by using Al-33Cu eutectic as the base metal because the lowest achievable liquidus temperature of aluminum alloys is the eutectic temperature 548°C. An advantage of selecting Al-33Cu eutectic as the base metal is that its lamellar microstructure is easy to recognize. 1100 Al was used as the filler metal to keep the weld-metal Cu content as low as possible, that is, T_{LW} as high as possible. In one experiment the weld-metal Cu content was further reduced by placing before welding a rectangular rod of 1100 Al in a rectangular groove at the workpiece top surface along the welding path.

Figure 7 shows longitudinal micrographs taken along the central plane of a weld made on Al-33Cu eutectic with filler metal 1100 Al. The eutectic had been heat treated at 540°C for 65 h before welding to develop a spherodized eutectic microstructure. This was intended to enhance the contrast between the base metal and the beach along the weld interface, which was expected to be also eutectic but much finer and lamellar, typical of an as-solidified eutectic.

Figure 7A shows the overall microstructure along the bottom of the weld, the welding direction being from right to left. Figure 7B shows the microstructure somewhere along the melting front, as can be seen from the rising fusion boundary from right to left. Figure 7C and D show, respectively, some peninsulas and one island at a higher magnification.

The dilution was 67.3%, and the composition of the bulk weld metal was Al-24Cu. From the Al-Cu phase diagram, T_{LW} = 586°C and T_{LB} = 548°C. An advantage for selecting Al-33Cu eutectic as the base metal is that the condition of $T_{LW} > T_{LB}$ is met automatically. Another advantage is that the eutectic is distinctly different from other Al-Cu alloys in microstructure and hence easy to recognize.

Figure 7B shows a beach thick and continuous along the fusion boundary at the melting front. At higher magnifications, the beaches exhibited a lamellar structure, typical of as-cast eutectic. According to the proposed mechanism (Ref. 18), complete mixing throughout the weld pool is impossible because $T_{LW} > T_{LB}$. Thus, a continuous layer of liquid base metal exists along the melting front, regardless of the extent of weld pool convection, and solidifies into a beach continuous along the resultant fusion boundary. The presence of the eutectic beach along the fusion boundary at the melting front is consistent with the proposed mechanism, in that complete mixing is impossible when $T_{LW} > T_{LB}$. The interface between the unmelted base metal and the eutectic beach was at the eutectic temperature, suggesting that the melting front was at the liquidus temperature of the base metal T_{LB} (the eutectic temperature in this case) instead of the liquidus temperature of the weld metal T_{LW}. This is also consistent with the proposed mechanism.

As shown in Fig. 7C, the weld metal intruded into the beach along the fusion boundary. The beach was continuous and the peninsulas were randomly oriented, instead of being roughly parallel to the fusion boundary as in the case of $T_{LW} < T_{LB}$. This is also consistent with the proposed mechanism. Both the island and the beach in Fig. 7D were eutectic, as confirmed by microstructure examination at higher magnifications.

Thus, the beach, peninsulas, and island in Fig. 7 were all eutectic just like the base metal itself. As such, they all originated from the liquid base metal near the pool boundary that did not mix with the liquid weld metal. The peninsulas and the island were the liquid base metal left in the space between the weld-metal intrusions that solidified without mixing, as suggested by Mechanism 2.

Before leaving Fig. 7, it is worth mentioning that, as shown in Fig. 7A, the weld penetration appears to fluctuate significantly. The so-called papillary penetration is common in partial-penetration welding of Al alloys with Ar as the shielding gas, such as in the present study. The penetration tip tends to fluctuate up and down along the weld (Refs. 23, 24).

Figure 8 shows the transverse micrographs of two welds made on as-cast Al-33Cu eutectic with filler metal 1100 Al. The first micrograph (Fig. 8A) was taken from the weld made with a 66.5% dilution, and the weld metal composition was Al-23.8Cu. From the Al-Cu phase diagram, T_{LB} = 548°C and T_{LW} = 586°C. Thus, T_{LW} was above T_{LB} and ($T_{LW} - T_{LB}$) = 38°C.

The beach was continuous along the fusion boundary but intruded by the weld metal at multiple locations along the fusion boundary. Peninsulas and islands of random orientations existed in the space between intrusions. The beach, peninsulas, and islands had a lamellar structure characteristic of the eutectic alloy just like the eutectic base metal (as can be seen in Fig. 9B). These observations are consistent with Mechanism 2.

The second micrograph (Fig. 8B) was taken from another weld made on as-cast Al-33Cu with filler metal 1100 Al. A rectangular rod of 1100 Al was placed in a rectangular groove machined at the top of the workpiece before welding in order to further reduce the weld-metal Cu content and raise the temperature difference ($T_{LW} - T_{LB}$). Microstructural examination of

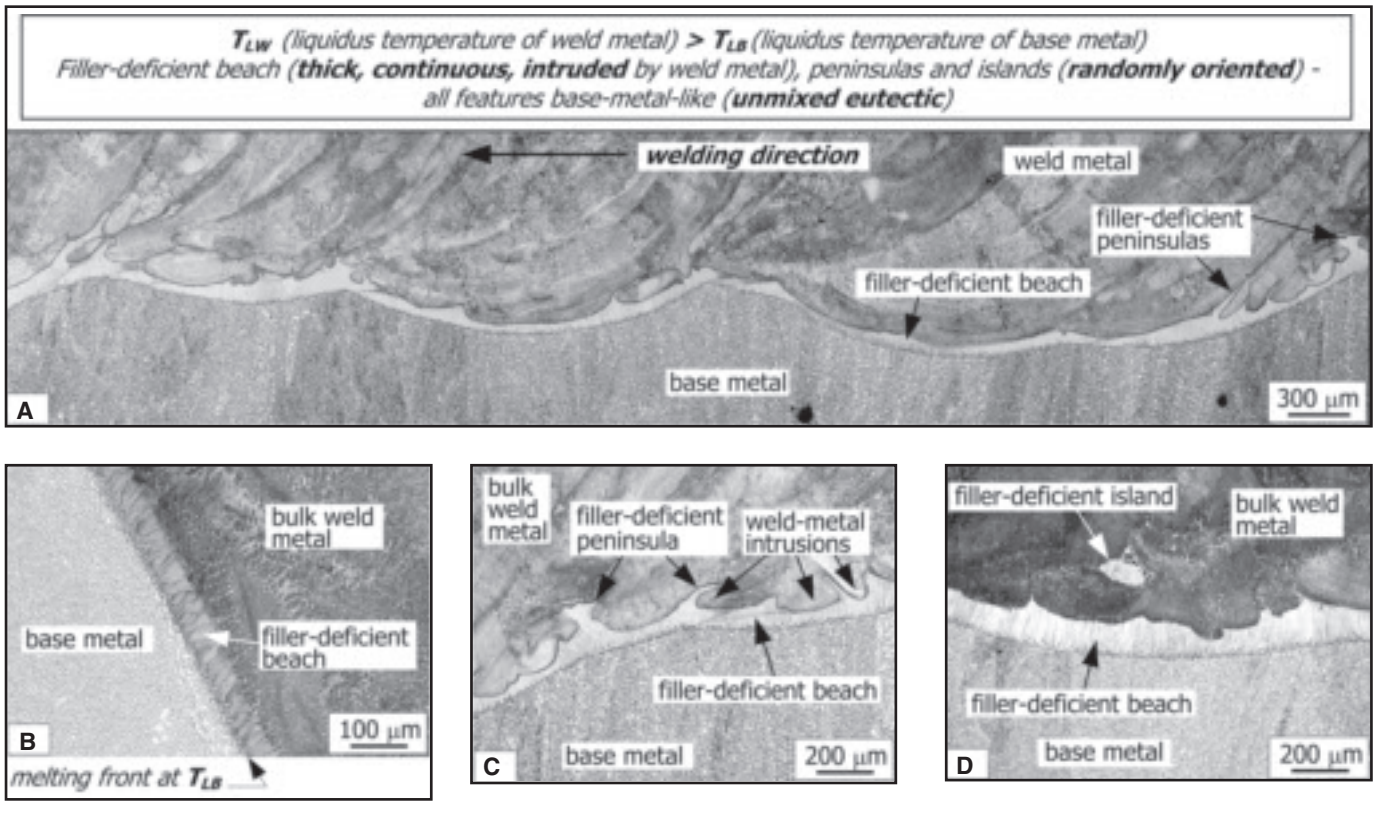

Fig. 7 — Longitudinal micrographs for $T_{LW} > T_{LB}$. A — Overview; B — melting front; C, D — weld bottom. Base metal: Al-33Cu (eutectic, heat-treated); weld metal: Al-24Cu. T_{LW} = 586°C and T_{LB} = 548°C. At higher magnifications, beach, peninsulas, and island all appeared eutectic (but lamellar) like base metal, suggesting they originated from unmixed base metal.

the resultant weld confirmed that the rod was completely melted and mixed with the bulk weld pool. The weld metal composition was Al-16Cu based on the compositions of the base and filler metals and the weld transverse cross section, which showed the contributions to the weld metal were 41.6% from the base metal (the dilution), 40.6% from the filler metal, and 17.8% from the rod. From the Al-Cu phase diagram, T_{LB} = 548°C, T_{LW} = 613°C, and thus, ($T_{LW} - T_{LB}$) was raised to 65°C.

The beach in the second weld (Fig. 8B) was also eutectic like that in the first weld but much thicker. This difference is consistent with Mechanism 2, which suggests that with a larger ($T_{LW} - T_{LB}$), a thicker unmixed zone is likely to exist. However, it is possible that the 1100 Al rod, with its higher liquidus temperature and hence greater resistance to melting, could have slowed down the velocity of the liquid weld metal induced by the filler-metal droplets and helped a thick layer of liquid base metal survive and thus further contributed to a thick filler-deficient beach.

Figure 9 shows the transverse micrographs of a weld made on as-cast Al-33Cu eutectic with filler metal 1100 Al. The dilution was 56.3%, and the weld metal composition was Al-20.7Cu. From the Al-Cu phase diagram, T_{LB} = 548°C and T_{LW} = 598°C. Thus, T_{LW} was above T_{LB} and ($T_{LW} - T_{LB}$) = 50°C. The beach is continuous along the fusion boundary but intruded by the weld metal — Fig. 9A. A section of the beach near the upper-right corner of the micrograph is shown at a higher magnification — Fig. 9B. The microstructure of the beach is lamellar, typical of as-cast eutectic just like the base metal itself. This clearly suggests that the beach originated from the layer of the liquid base metal along the pool boundary that solidified without mixing with the liquid weld metal.

In general, the lamellar structure in the beach was too fine to reveal clearly at a magnification level (e.g., 300×) that was kept low enough in order to include the beach, bulk weld metal, and base metal all in one micrograph. Only a few columnar eutectic grains were oriented such that their α-Al and θ-Al_2Cu layers were at the best angle to show the lamellar structure more clearly. At higher magnifications (e.g., 1000×), however, all grains in the beach exhibited a clear lamellar structure.

A composition profile (Fig. 9C) was taken along path A–D (Fig. 9B) across the fusion boundary. It shows that the Cu content was uniform at about Al-35Cu across the beach just like the base metal. This is essentially the eutectic composition of Al-33Cu. This further confirms that the beach was an unmixed liquid base metal.

This composition profile also shows another advantage of selecting eutectic Al-33Cu as the base metal, that is, the composition profile in the eutectic (including the base metal and the beach) is easy to measure by EDS because it is essentially uniform. On the contrary, the composition in the weld metal fluctuated wildly between the eutectic composition of about 33% Cu when the electron beam hit the interdendritic eutectic and the α-Al composition of about 6% Cu when the beam hit the dendrite arms. The dashed line represents the average weld metal composition of Al-20.7Cu mentioned previously.

Conclusions

The present study was conducted to verify the mechanisms proposed recently for fusion-boundary macrosegregation in arc welds made with dissimilar filler metals (Ref. 18). Al-Cu welds were made by gas metal arc welding with dissimilar filler metals. The filler metals made the liquidus temperature of the weld metal T_{LW} different from that of the base metal T_{LB}. Two groups of welds were made. In the first

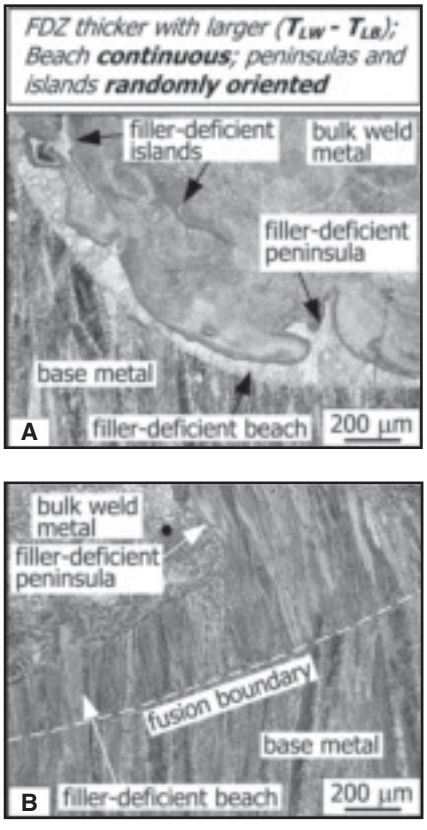

Fig. 8 — Transverse micrographs showing effect of (T_{LW} – T_{LB}) on thickness of filler metal-deficient zone (FDZ): A — (T_{LW} – T_{LB}) = 38°C; B — (T_{LW} – T_{LB}) = 65°C. Base metal: as-cast Al-33Cu (eutectic).

group, the dissimilar filler metal made $T_{LW} < T_{LB}$ and in the second group $T_{LW} > T_{LB}$. The microstructure and composition profiles near the fusion boundary of the resultant welds were examined. The conclusions are as follows:

1) The Al-Cu welds made with dissimilar filler metals have shown along the fusion boundary features including beaches, peninsulas, and islands essentially identical to the base metal both in microstructure and composition, both when $T_{LW} < T_{LB}$ and $T_{LW} > T_{LB}$. This demonstrates that these filler-deficient features originated from the liquid base metal that did not mix with the bulk weld pool, to which the dissimilar filler metal was added. According to the proposed mechanisms, such filler-deficient features can form due to lack of mixing between the layer of liquid base metal along the pool boundary and the bulk weld pool, both when $T_{LW} < T_{LB}$ and $T_{LW} > T_{LB}$. The layer can exist because convection is weakened near the pool boundary when $T_{LW} < T_{LB}$ but always exists regardless of convection when $T_{LW} > T_{LB}$.

2) The Al-Cu welds made with dissimilar filler metals have shown a thicker filler-deficient zone in welds made with a larger difference between T_{LW} and T_{LB}, both when $T_{LW} < T_{LB}$ and $T_{LW} > T_{LB}$. The proposed mechanism suggests that the filler-deficient zone can be thicker with a larger difference between T_{LW} and T_{LB}, both when $T_{LW} < T_{LB}$ and $T_{LW} > T_{LB}$, but the actual thickness can be affected by the strength and direction of convection in the weld pool.

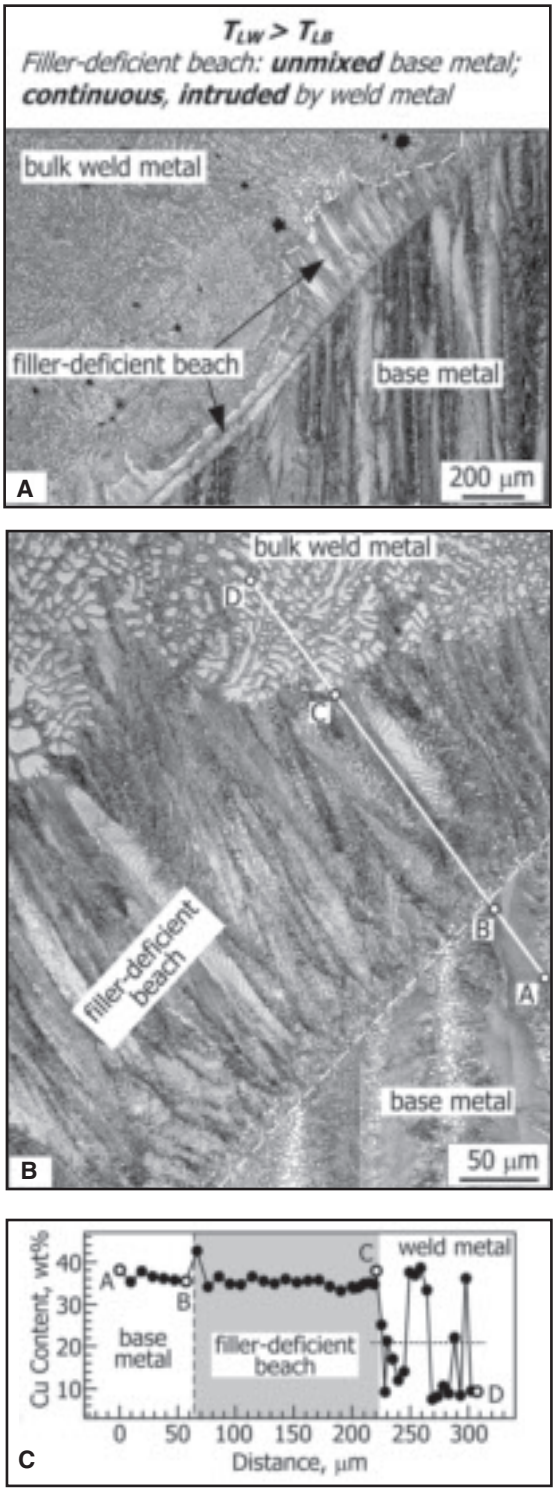

Fig. 9 — Macrosegregation across fusion boundary when $T_{LW} > T_{LB}$. A — Transverse micrographs; B — enlarged; C — composition profile. Base metal: as-cast Al-33Cu (eutectic). Beach identical to base metal in composition, i.e., unmixed base metal.

3) The Al-Cu welds made with $T_{LW} < T_{LB}$ have shown filler-metal-deficient beaches thin and discontinuous along the fusion boundary, and filler-deficient peninsulas and islands roughly parallel to the fusion boundary. According to Mechanism 1 for $T_{LW} < T_{LB}$, the region of liquid weld metal immediately ahead of the T_{LW} solidification front is below T_{LB} and thus cooler than the liquid base metal and that the liquid base metal swept from the layer into the region can freeze quickly as peninsulas or islands without much mixing with the liquid weld metal. The liquid base metal remaining in the layer, which is thin and discontinuous because of weld pool convection, can solidify into a thin and discontinuous beach.

4) The Al-Cu welds made with $T_{LW} > T_{LB}$ have shown along the fusion boundary a thick continuous filler-deficient beach that is intruded by the weld metal, and filler-deficient peninsulas and islands that are randomly oriented. The proposed mechanism for $T_{LW} > T_{LB}$ suggests that the layer of liquid base metal is below T_{LW} and thus cooler than the liquid weld metal and that the liquid weld metal pushed by convection into the layer can freeze quickly into weld-metal intrusions without much mixing with the liquid base metal. The liquid base metal in the space between the intrusions solidifies in random orientations. Since the layer must exist regardless of weld pool convection, it can be thick and continuous and thus can solidify into a thick and continuous beach.

5) Conclusions 1–4 show that the proposed mechanisms have been verified by the Al-Cu welds made with dissimilar filler metals.

6) The present study can help guide the selection of filler metals to minimize macrosegregation near the fusion boundary in dissimilar-filler welding. First, a filler metal that makes a smaller change in the liquidus temperature of the weld metal is likely to

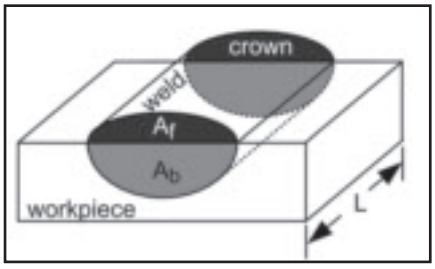

Fig. A1 — Schematic showing a section of the weld (L), the area representing the contribution of the base metal to the weld metal (A_b), and the area representing the contribution of the filler metal to the weld metal (A_f), that is, the transverse cross-sectional area of the crown.

cause less macrosegregation. Second, for the same absolute value of $(T_{LW} - T_{LB})$, a filler metal that lowers the liquidus temperature of the weld metal (that is, $T_{LW} < T_{LB}$) is likely to cause less macrosegregation than a filler metal that raises the liquidus temperature of the weld metal (that is, $T_{LW} > T_{LB}$).

7) The Al-Cu system is a useful alloy system for studying solidification and macrosegregation in dissimilar-filler welds. The easy-to-recognize microstructures and easy-to-measure compositions of pure Al and Al-33Cu eutectic are particularly helpful.

Acknowledgments

This work was supported by National Science Foundation under Grant No. DMR-0455484. The authors are grateful to Bruce Albrecht and Todd Holverson of Miller Electric Manufacturing Co., Appleton, Wis., for donating the welding equipment, which included an Invision 456P power source, and an XR-M wire feeder and gun.

Appendix A

Figure A1 shows L the length of the weld, A_b the area representing the contribution of the base metal to the weld metal, and A_f the area representing the contribution of the filler metal to the weld metal.

$$\text{Weight of Cu in weld from base metal} = (\text{vol-\% Cu})_{base} A_b L \rho_{Cu} = \{(\text{wt-\% Cu} / \rho_{Cu}) / [\text{wt-\% Cu} / \rho_{Cu} + (100 - \text{wt-\% Cu}) / \rho_{Al}]\}_{base} A_b L \rho_{Cu} \quad \text{(A1)}$$

$$\text{Weight of Cu in weld from filler metal} = (\text{vol-\% Cu})_{filler} A_f L \rho_{Cu} = \{(\text{wt-\% Cu} / \rho_{Cu}) / [\text{wt-\% Cu} / \rho_{Cu} + (100 - \text{wt-\% Cu}) / \rho_{Al}]\}_{filler} A_f L \rho_{Cu} \quad \text{(A2)}$$

$$\text{Weight of Cu in weld} = (\text{vol-\% Cu})_{weld} (A_b + A_f) L \rho_{Cu} = \{(\text{wt-\% Cu} / \rho_{Cu}) / [(\text{wt-\% Cu} / \rho_{Cu}) + (100 - \text{wt-\% Cu}) / \rho_{Al}]\}_{weld} (A_b + A_f) L \rho_{Cu} \quad \text{(A3)}$$

$$\text{Weight of Cu in weld} = \text{weight of Cu in weld from base metal} + \text{weight of Cu in weld from filler metal} \quad \text{(A4)}$$

Equations A1–A4 can be solved simultaneously, and the result is Equation 2.

References

1. Houldcroft, R. T. 1954. Dilution and uniformity in aluminum alloy weld beads. *British Welding Journal* 1: 468–472.

2. Savage, W. F., and Szekeres, E. S. 1967. A mechanism for crack formation in HY-80 steel weldments. *Welding Journal* 46: 94-s to 96-s.

3. Savage, W. F., Nippes, E. F., and Szekeres, E. S. 1976. A study of fusion boundary phenomena in a low alloy steel. *Welding Journal* 55: 260-s to 268-s.

4. Duvall, D. S., and Owczarski, W. A. 1968. Fusion-line composition gradients in an arc-welded alloy. *Welding Journal* 47: 115-s to 120-s.

5. Karjalainen, L. P. 1979. Weld fusion boundary structures in aluminum and Al-Zn-Mg alloy. *Z. Metallkde*. 70: 686–689.

6. Doody, T. 1992. Intermediate mixed zones in dissimilar metal welds for sour service. *Welding Journal* 61: 55–60.

7. Omar, A. A. 1998. Effects of welding parameters on hard zone formation at dissimilar metal welds. *Welding Journal* 67: 86-s to 93-s.

8. Lippold, J. C., and Savage, W. F. 1980. Solidification of austenitic stainless steel weldments: Part 2 — The effect of alloy composition on ferrite morphology. *Welding Journal* 59: 48-s to 58-s.

9. Baeslack, W. A. III, Lippold, J. C., and Savage, W. F. 1979. Unmixed zone formation in austenitic stainless steel weldments. *Welding Journal* 58: 168-s to 176-s.

10. Ornath, F., Soudry, J., Weiss, B. Z., and Minkoff, I. 1991. Weld pool segregation during the welding of low alloy steels with austenitic electrodes. *Welding Journal* 60: 227-s to 230-s.

11. Albert, S. K., Gills, T. P. S., Tyagi, A. K., Mannan, S. L., Kulkarni, S. D., and Rodriguez, P. 1997. Soft zone formation in dissimilar welds between two Cr-Mo steels. *Welding Journal* 66: 135-s to 142-s.

12. Linnert, G. E. 1967. *Welding Metallurgy*, Vol. 2. American Welding Society, Miami, Fla.

13. Savage, W. F., Nippes, E. F., and Szekeres, E. S. 1976. Hydrogen-induced cold cracking in a low-alloy steel. *Welding Journal* 55: 276-s to 283-s.

14. Rowe, M. D., Nelson, T. W., and Lippold, J. C. 1999. Hydrogen-induced cracking along the fusion boundary of dissimilar metal welds. *Welding Journal* 78: 31-s to 37-s.

15. Kent, K. G. 1970. Weldable Al-Zn-Mg alloys. *Metals and Materials* 4: 429–440.

16. Cordier, H., Schippers, M., and Polmear, I. Microstructure and intercrystalline fracture in a weldable aluminum-zinc-magnesium alloy. *Z. Metallkde*. 68: 280–284.

17. Pirner, M., and Bichsel, H. Corrosion resistance of welded joints in AlZnMg. *Metall* 29: 275–280.

18. Kou, S., and Yang, Y. K. 2007. Fusion-boundary macrosegregation in dissimilar-filler welds. *Welding Journal* 86: 303-s to 312-s.

19. Kou, S. 2003. *Welding Metallurgy*, 2nd ed., Wiley, New York, N.Y., pp. 114, 180, 206, and 306.

20. American Society for Metals. 1986. Binary Alloy Phase Diagrams, vol. 1: p. 106, Materials Park, Ohio, ASM International.

21. Yang, Y. K., and Kou, S. 2007. Weld-bottom macrosegregation in dissimilar-filler welds. *Welding Journal* accepted.

22. Kou, S. 1996. *Transport Phenomena and Materials Processing*, John Wiley and Sons, New York, N.Y., pp. 57–60.

23. Huang, C., and Kou, S. 2003. Liquation cracking in partial-penetration aluminum welds: effect of penetration oscilation, and backfilling. *Welding Journal* 82: 184-s to 194-s.

24. Huang, C., Cao, G., and Kou, S. 2004. Liquation cracking in partial-penetration aluminum welds: assessing tendencies to liquate, crack and backfill. *Science and Technology of Welding and Joining*, 9, pp. 1–9.

ARTICLE REPRINTS

To order custom reprints of 100 or more of articles in *Welding Journal,* call FosteReprints at (219) 879-8366 or (800) 382-0808. Request for quotes can be faxed to (219) 874-2849. You can e-mail FosteReprints at *sales@fostereprints.com.*